IEEE Access
Multidisciplinary ⋮ Rapid Review ⋮ Open Access Journal

Received January 25, 2021, accepted February 2, 2021, date of publication February 10, 2021, date of current version February 25, 2021.

Digital Object Identifier 10.1109/ACCESS.2021.3058340

Performance Enhancement of MIMO Patch Antenna Using Parasitic Elements

HUY HUNG TRAN[1,2] AND NGHIA NGUYEN-TRONG[3], (Member, IEEE)

[1]Faculty of Electrical and Electronic Engineering, PHENIKAA University, Hanoi 12116, Vietnam
[2]PHENIKAA Research and Technology Institute (PRATI), A&A Green Phoenix Group JSC, Hanoi 11313, Vietnam
[3]School of Electrical and Electronic Engineering, The University of Adelaide, Adelaide, SA 5000, Australia

Corresponding author: Huy Hung Tran (hung.tranhuy@phenikaa-uni.edu.vn)

ABSTRACT This paper investigates the effects of parasitic elements on the performance of MIMO patch antenna. Multiple square parasitic elements are added in close proximity to each of the rectangular patch elements. These parasitic elements affect the electromagnetic field distribution and consequently reduce the mutual coupling. In addition, wider bandwidth is also achieved. Two MIMO antennas coupled in H-plane and E-plane are designed and measured to demonstrate the proposed concept. The measured results show that both designs have a wide impedance bandwidth of 14% with isolation of more than 20 dB across the whole band (with a small antenna profile of $0.05\lambda_0$). For 40-dB isolation, the H-coupled and E-coupled design achieve a bandwidth of 2.7% and 1.5%, respectively. Compared to other methods, the proposed method has much simpler structure, wider bandwidth and comparable improvement in isolation, with the tradeoff in larger antenna element size.

INDEX TERMS MIMO antenna system, high isolation, isolation enhancement techniques, microstrip patch antennas (MPA), parasitic elements, wideband antennas.

I. INTRODUCTION

Ehancing isolation among radiating elements is one of the most critical tasks in designing a multiple-input-multiple-output (MIMO) antenna system. Furthermore, a large number of MIMO systems are built with microstrip patch technology owing to its low cost, low profile and ease of integration. Thus, the literature on improving isolation in patch antenna arrays is notably rich with numerous methods being proposed. Based on the difference on the design structures, those methods can be broadly characterized in several categories: (i) using defected ground structure (DGS) [1]–[6], (ii) adding sophisticated decoupling structures (without disturbing the ground plane) [7]–[18], (iii) adding near-field resonant structures (on top of the antennas) [19]–[21], and (iv) other unconventional methods [22], [23]. For DGS, the main disadvantage is the disturbance on the ground plane. This reduces the integration capability of the design on multi-layered electronic circuits because there must be free-space underground plane for the DGS to operate. Other decoupling structures may have the disadvantage of having a 3D structure [7], [14]. The near-field resonant structures mostly increase the design height profile [19]–[21]. The unconventional method in [22] is based on the weak-field region of the patch, which may be limited on the selection of the feeding structure. The method in [23] significantly increases the antenna size in both planar and vertical dimension. Finally, almost all methods require some degrees of complicated structures to be added.

This letter examines a very simple method of adding parasitic patch elements. In terms of design structure, this method has critical advantages of maintaining the low profile and do not disturb the ground plane. In terms of performance, the antenna bandwidth (BW) is significantly improved while the enhancement in isolation is comparable with other methods. Nevertheless, there is some limitation in applying the proposed method in a larger array. This paper will perform a systematic investigation on this technique to illustrate its advantages and disadvantages.

Since a linear patch array can be arranged in H-plane or E-plane coupled configuration, Section II and III will investigate H-plane and E-plane coupled array, respectively. It is noted that we do not consider the situation where the patches are arranged orthogonally to achieve orthogonal polarization,

The associate editor coordinating the review of this manuscript and approving it for publication was Lei Ge.

such as in [24], since this method is limited in the configuration of the elements. A thorough comparison with other methods is provided in Section IV, followed by a conclusion in Section V.

II. H-PLANE COUPLED MIMO PATCH ANTENNA

A. ANTENNA CONFIGURATION

Fig. 1 shows the geometrical configuration of the H-planed coupled MIMO antenna with parasitic elements. The antenna is fabricated on a low-loss Taconic TLY substrate ($\epsilon_r = 2.2$, thickness $H_s = 1.57$ mm, loss tangent $\tan\delta = 0.0009$). The primary radiators are two rectangular patches that are in close proximity to four square patches as parasitic elements. For simplicity, the antennas are excited by two 50-Ω coaxial connectors; nevertheless, other types of feed can also be used.

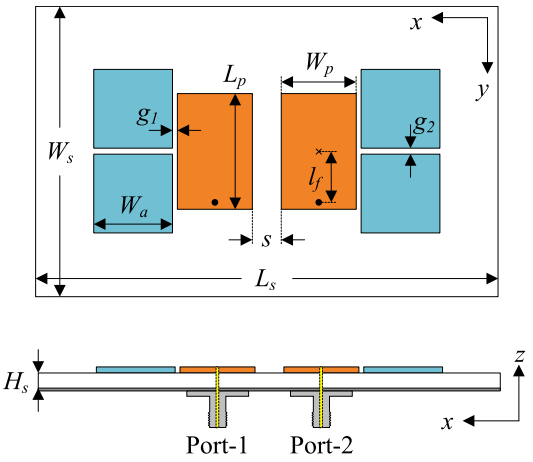

FIGURE 1. Geometry of the H-coupled MIMO patch antenna with parasitic elements to enhance the isolation. The optimized dimensions are $L_S = 80$, $W_S = 50$, $L_P = 20$, $W_P = 13$, $l_f = 8.5$, $W_a = 13.6$, $g_1 = 0.8$, $g_2 = 0.9$, $s = 5$ (unit: mm).

B. OPERATING MECHANISM

To understand the effects of the parasitic elements, four configurations of MIMO antennas are investigated (Fig. 2) with performances shown in Fig. 3. For the antenna without parasitic element (Antenna-H1), the impedance BW is quite small, i.e. about 4%, which is typical of a simple patch antenna (Fig. 3(a)). Besides, poor isolation is observed within this band, which is worse than 10 dB. Again, this is typical with a spacing s of only about $0.09\lambda_0$ where λ_0 is the free-space wavelength at the center frequency.

When the parasitic elements are introduced, the operating BW, isolation, and realized gain are significantly improved. In terms of reflection coefficient, the parasitic elements produce additional resonance in the higher frequency range, which combines with the lower resonance generated by the driven patch to broaden the overall −10-dB impedance BW of the antenna. For the isolation response, the antennas with parasitic elements show much better performance than those without parasitic elements. Furthermore, more parasitic elements result in better gain radiation.

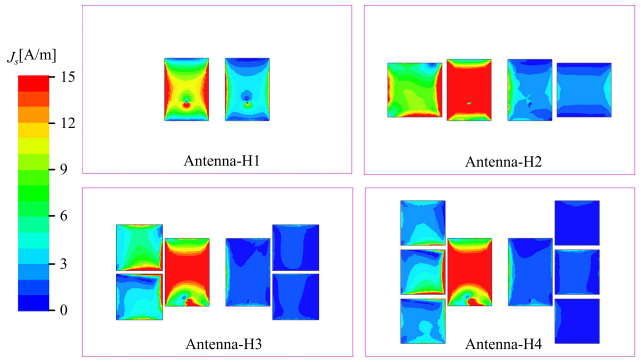

FIGURE 2. Different configurations of H-coupled MIMO patch antenna and their simulated surface current distributions at 5.4 GHz.

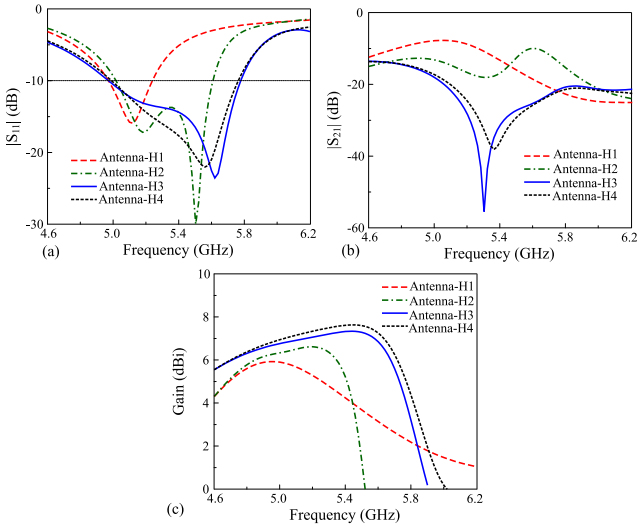

FIGURE 3. Simulated (a) $|S_{11}|$, (b) $|S_{21}|$, and (c) gain of Antenna-H1, -H2, -H3, and -H4.

The gain and isolation improvements can be explained based on the simulated current distributions (Fig. 2). When the parasitic elements are introduced, the power from the excited patch tends to couple with the parasitic elements rather than the non-excited patch, resulting in mutual coupling reduction. Depending on the number and position of the parasitic elements, the couplings are different. Here, the best isolation performance is achieved with Antenna-H3 as confirmed from the simulated current in Fig. 2 and performance in Fig. 3(b). The isolation enhancement is expected as the parasitic elements effectively increase the distance between the two antenna elements (the phase center of each radiating element is moved further away from each other). In terms of gain, higher gain values are obtained for the antenna with more parasitic elements, which is simply due to the larger radiating aperture.

In fact, the gain and BW improvement for patch antenna with parasitic elements are well known [25]–[28]. However, we demonstrate these features in this letter together with the effect on isolation. It is interesting to observe that all antenna characteristics are improved significantly by simply adding several additional patches without any further complication

in feeding. Nevertheless, this technique increases the overall antenna size and may not be applicable for more-than-two-element array. A more attractive case on E-coupled MIMO antenna will be investigated in Section III.

C. MEASUREMENT RESULTS

The measured S-parameter of the H-coupled MIMO antenna (Antenna-H3) is shown in Fig. 4. The antenna has a wide –10-dB impedance BW of 14.8% (5.0–5.8 GHz). Within this band, the isolation is better than 20 dB. For a BW of 2.7% (5.13-5.27 GHz), an isolation of more than 40 dB is obtained. The realized gain in the band 5.0-5.8 GHz is higher than 3.8 dBi. The envelop correlation coefficient (ECC) is around 0.02 (Fig. 5(a) and (b)). Since this antenna has high efficiency (simulated value of better than 95%), the ECC calculation from both pattern and S-parameters are close to each other. The radiation patterns at 5.2 GHz are plotted in Fig. 5(c) with polarization isolation of about 12 dB at broadside.

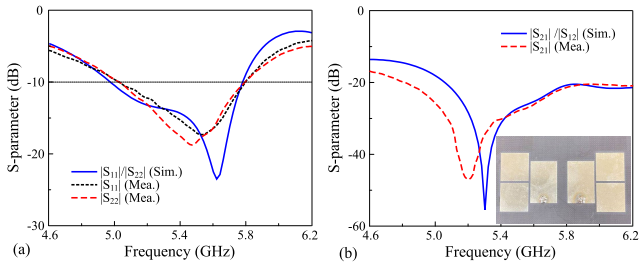

FIGURE 4. (a) Reflection coefficient and (b) isolation of the proposed H-coupled MIMO antenna (photograph of prototype shown in the inset).

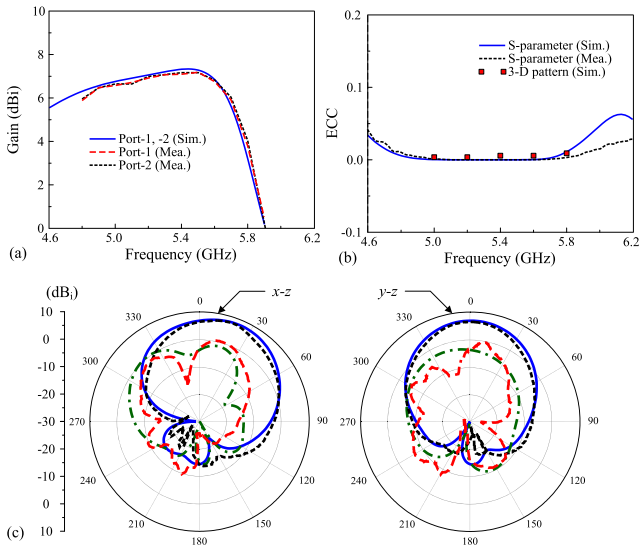

FIGURE 5. (a) Gain, (b) ECC, (c) Radiation pattern at 5.2 GHz of the H-coupled MIMO antenna.

III. E-PLANE COUPLED MIMO ANTENNA

A. ANTENNA CONFIGURATION

The geometry of a two-element E-plane coupled MIMO patch antenna with parasitic elements is shown in Fig. 6. In this

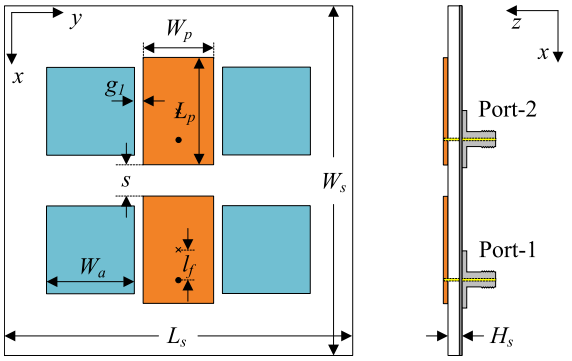

FIGURE 6. Geometry of the proposed E-coupled MIMO antenna. The optimized dimensions are $L_s = 60$, $W_s = 60$, $L_p = 18.4$, $W_p = 12$, $l_f = 5$, $W_a = 15.2$, $g_1 = 1.6$, $s = 5$ (unit: mm).

case, the parasitic elements can be positioned on both sides of the driven patch for a symmetrical geometry and better mutual coupling reduction. In this configuration, the center spacing between two elements remain the same.

B. OPERATING MECHANISM

Similar to the previous case, Fig. 7 shows the steps taken to realize the final antenna and Fig. 8 presents the operation characteristics of these designs. As expected, Antenna-E1 without parasitic elements exhibits narrow BW and poor isolation. When the parasitic elements are added only in one side of the driven patch, a wider BW can be obtained for Antenna-E2. In addition, the mutual coupling between MIMO elements is significantly reduced. For better isolation, more parasitic elements are utilized as Antenna-E3. In this case, the isolation within the operating BW is always better than 20 dB. An isolation of better than 40 dB is obtained in the BW of 1.1% (5.34-5.40 GHz).

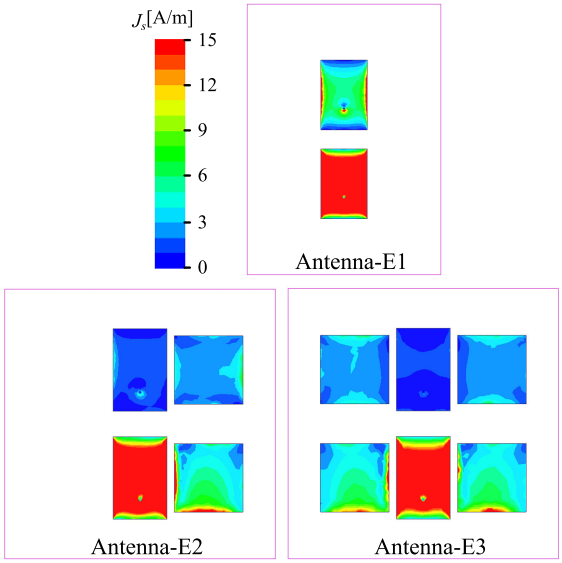

FIGURE 7. Simulated surface current distributions at 5.4 GHz of Antenna-E1, -E2, and -E3.

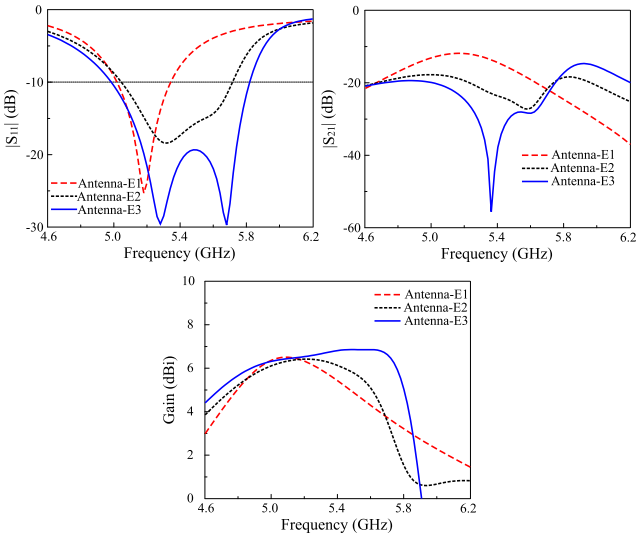

FIGURE 8. Simulated (a) $|S_{11}|$, (b) $|S_{21}|$, and (c) gain of Antenna-E1, -E2, and -E3.

As confirmed from the simulated surface current in Fig. 7, the antenna without parasitic elements has strong coupling from the excited patch to the other. Meanwhile, more power is coupled to the parasitic elements for Antenna-E2 and -E3. Interestingly, in this case, the effective distance between two radiating elements remain the same (as parasitic elements are only added to the side of the patch); however, the isolation is still improved due to the fact that more power is coupled with the parasitic patches. This makes the method extendable to a larger array as will be shown in Section III.D.

C. MEASUREMENT RESULTS

Fig. 9 shows the simulated and measured S-parameter of the E-coupled MIMO antenna (Antenna-E3). It achieves a –10-dB impedance BW of 14.8% (5.0–5.8 GHz) with an isolation of better than 20 dB across this band. For 40-dB isolation, a relative BW of 1.5% (5.26-5.34 GHz) is obtained. Meanwhile, the realized gain is in the range from 5.2 to 6.8 dBi and the ECC value is around 0.02 (Fig. 10(a) and (b)). The radiation patterns at 5.2 GHz are plotted in Fig. 10(c). It can be seen that the patterns are symmetric around the broadside direction. The polarization isolation and front-to-back ration are better than 40 dB and 22 dB, respectively. Compared to H-plane coupled design, the cross polarization for this design is much lower due to the symmetry of the structure.

D. MULTIPLE ELEMENT ARRAY

Since the center spacing between two elements remains the same in this case, the method can also be applied for multi-element patch arrays. For demonstration, Fig. 11 shows the geometry of three-element MIMO antenna and its simulated S-parameters. It can be seen that the multi-element MIMO is capable of exhibiting wideband operation with high-performance isolation characteristic. Here, the –10-dB impedance BW is from 5.06 to 5.72 GHz, corresponding

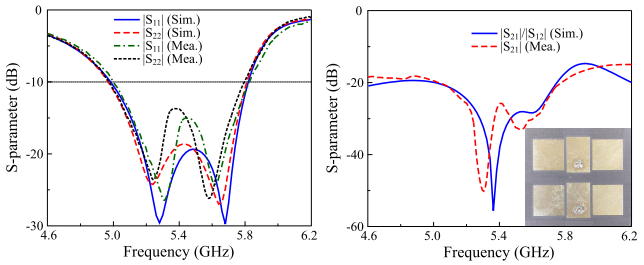

FIGURE 9. (a) Reflection coefficient and (b) isolation of the proposed E-coupled MIMO antenna (photograph of prototype shown in the inset).

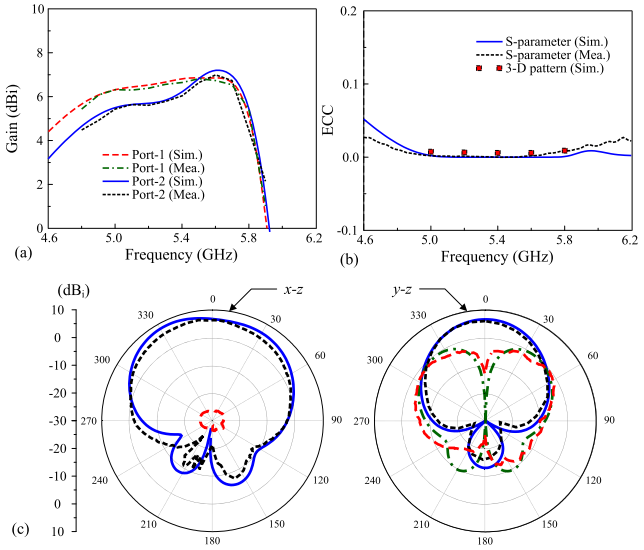

FIGURE 10. (a) Gain, (b) ECC and (c) Radiation pattern at 5.2 GHz of the E-coupled MIMO antenna.

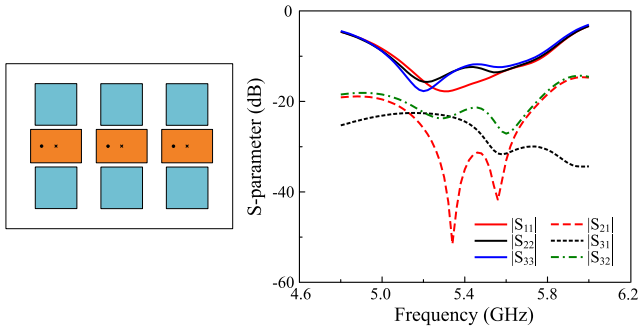

FIGURE 11. S-parameter of the multi-element E-plane coupled MIMO antenna.

to 12.2%. Meanwhile, the isolation within this band is always better than 20 dB. Based on all presented results through Section II and III, it is expected that the proposed method can be applicable for a $2 \times N$ array (N can be larger than 2) where there are two elements in H-plane and N elements in E-plane with some constraints on the element spacing.

IV. PERFORMANCE COMPARISON

Comparison on the merits of different methods for isolation enhancement is not straightforward as many factors can affect

TABLE 1. Performance comparison among microstrip patch MIMO antenna.

Ref.	Method	Edge Spacing (λ_0)	Center Spacing (λ_0)	Profile (λ_0)	Coupled Plane	−10-dB Impedance BW (%)	20-dB Iso. BW (%)	40-dB Iso. BW (%)
[1]	DGS	0.04	0.26	0.02	E-plane	< 3.0	< 3.0	N/A
[2]	DGS	0.17	0.34	0.06	E-plane	< 3.0	< 3.0	< 0.5
[3]	DGS	0.03	0.31	0.02	H-plane	< 3.0	< 3.0	< 0.5
[6]	DGS & Decoupling Structure	0.06	0.31	0.03	H-plane	< 3.0	< 3.0	N/A
[7]	Decoupling Structure	0.03	0.28	0.23	H-plane	< 3.0	< 3.0	N/A
[8]	Decoupling Structure	0.07	0.30	0.03	H-plane	< 3.0	< 3.0	N/A
[10]	Decoupling Structure	0	0.76	0.04	E, H-plane	16	16	N/A
[14]	Decoupling Structure	0.31	> 0.50	0.18	E, H-plane	8.7	8.7	N/A
[21]	Near-field Resonator	0.04	0.30, 0.58	0.05	E, H-plane	6.0	6.0	< 0.5
[22]	Weak-field Area	0.18	0.50	0.04	E-plane	< 3.0	< 3.0	< 0.5
Prop.	Parasitic element	0.09	0.43, 0.58	0.05	E, H-plane	14.8	14.8	1.5, 2.7

the antenna performance. A higher profile tends to give larger BW. Smaller edge spacing and center spacing should yield worse isolation. Coupling in E and H-plane can be different. Since this paper focuses on improving the antenna BW, we present in Table 1all aforementioned factors together with the BW for different criteria on the matching and isolation.

It can be seen that for very small center spacing and small profile, it is extremely challenging to achieve large BW and high isolation as seen from the performance of [1]–[3], [7], [8]. For a larger center spacing, the performance of the proposed designs is quite attractive, compared to [10], [14], [21], [22]. Our method can achieve a much larger BW with a small profile of $0.05\lambda_0$ and similar center spacing (λ_0 is the free-space wavelength at the center frequency of impedance BW). Furthermore, the method also has a significant advantage of being easy to apply with simple structure and no disturbance on the ground plane.

The main disadvantage is the increasing size of the antenna with parasitic elements. It is noted that several methods, such as [10], [23], also significantly increase the antenna size (the design in [23] was also designed with two-element array). Furthermore, in this paper, we only examine a simple rectangular patch as parasitic elements. The method might be further investigated with different structures of parasitic elements, which can potentially reduce the size of the antenna. Finally, although the method has its limited applicability on a large array, it can still be applicable for a $2 \times N$ array (N can be larger than 2) by combining both proposed designs in Section II and III.

V. CONCLUSION

This paper examines a simple method of using parasitic elements to improve the performance of the MIMO patch antenna. By arranging parasitic elements in proper position, significant enhancements in operating BW, isolation, as well as realized gain are achieved. The proposed method has been applied to both two-element H-coupled and multi-element E-coupled MIMO antennas. Both designs show a much better performance in terms of operating BW and isolation, compared to other designs with similar center spacing.

REFERENCES

[1] Z. Niu, H. Zhang, Q. Chen, and T. Zhong, "Isolation enhancement for 1×3 closely spaced E-plane patch antenna array using defect ground structure and metal-vias," *IEEE Access*, vol. 7, pp. 119375–119383, 2019.

[2] K. Wei, J.-Y. Li, L. Wang, Z.-J. Xing, and R. Xu, "Mutual coupling reduction by novel fractal defected ground structure bandgap filter," *IEEE Trans. Antennas Propag.*, vol. 64, no. 10, pp. 4328–4335, Oct. 2016.

[3] A. A. Ghannad, M. Khalily, P. Xiao, R. Tafazolli, and A. A. Kishk, "Enhanced matching and vialess decoupling of nearby patch antennas for MIMO system," *IEEE Antennas Wireless Propag. Lett.*, vol. 18, no. 6, pp. 1066–1070, Jun. 2019.

[4] E. Fritz-Andrade, A. Perez-Miguel, R. Gomez-Villanueva, and H. Jardon-Aguilar, "Characteristic mode analysis applied to reduce the mutual coupling of a four-element patch MIMO antenna using a defected ground structure," *IET Microw., Antennas Propag.*, vol. 14, no. 2, pp. 215–226, Feb. 2020.

[5] G. Zhang and Q. Chen, "Mutual coupling reduction in Chinese character-shaped artistic MIMO antenna," *Microw. Opt. Technol. Lett.*, vol. 62, no. 7, pp. 2588–2594, Jul. 2020.

[6] C. Lu, Q. Zhang, H. Qi, S. Li, H. Zhao, and X. Yin, "Compact postwall slotline-based stepped impedance resonator decoupling structure for isolation enhancement of patch antenna array," *IEEE Antennas Wireless Propag. Lett.*, vol. 18, no. 12, pp. 2647–2651, Dec. 2019.

[7] H. Qi, L. Liu, X. Yin, H. Zhao, and W. J. Kulesza, "Mutual coupling suppression between two closely spaced microstrip antennas with an asymmetrical coplanar strip wall," *IEEE Antennas Wireless Propag. Lett.*, vol. 15, pp. 191–194, 2016.

[8] H. Qi, X. Yin, L. Liu, Y. Rong, and H. Qian, "Improving isolation between closely spaced patch antennas using interdigital lines," *IEEE Antennas Wireless Propag. Lett.*, vol. 15, pp. 286–289, 2016.

[9] S. Maddio, G. Pelosi, M. Righini, S. Selleri, and I. Vecchi, "Mutual coupling reduction in multilayer patch antennas via meander line parasites," *Electron. Lett.*, vol. 54, no. 15, pp. 922–924, Jul. 2018.

[10] K. D. Xu, J. Zhu, S. Liao, and Q. Xue, "Wideband patch antenna using multiple parasitic patches and its array application with mutual coupling reduction," *IEEE Access*, vol. 6, pp. 42497–42506, 2018.

[11] S. D. Assimonis, T. V. Yioultsis, and C. S. Antonopoulos, "Design and optimization of uniplanar EBG structures for low profile antenna applications and mutual coupling reduction," *IEEE Trans. Antennas Propag.*, vol. 60, no. 10, pp. 4944–4949, Oct. 2012.

[12] H. S. Farahani, M. Veysi, M. Kamyab, and A. Tadjalli, "Mutual coupling reduction in patch antenna arrays using a UC-EBG superstrate," *IEEE Antennas Wireless Propag. Lett.*, vol. 9, pp. 57–59, 2010.

[13] Z. Qamar, U. Naeem, S. A. Khan, M. Chongcheawchamnan, and M. F. Shafique, "Mutual coupling reduction for high-performance densely packed patch antenna arrays on finite substrate," *IEEE Trans. Antennas Propag.*, vol. 64, no. 5, pp. 1653–1660, May 2016.
[14] M.-C. Tang, Z. Chen, H. Wang, M. Li, B. Luo, J. Wang, Z. Shi, and R. W. Ziolkowski, "Mutual coupling reduction using meta-structures for wideband, dual-polarized, and high-density patch arrays," *IEEE Trans. Antennas Propag.*, vol. 65, no. 8, pp. 3986–3998, Aug. 2017.
[15] A. Abdelaziz and E. K. I. Hamad, "Isolation enhancement of 5G multiple-input multiple-output microstrip patch antenna using metamaterials and the theory of characteristic modes," *Int. J. RF Microw. Comput.-Aided Eng.*, vol. 30, no. 11, Nov. 2020, Art. no. e22416.
[16] R. Mark, H. V. Singh, K. Mandal, and S. Das, "Reduced edge-to-edge spaced MIMO antenna using parallel coupled line resonator for WLAN applications," *Microw. Opt. Technol. Lett.*, vol. 61, no. 10, pp. 2374–2380, Oct. 2019.
[17] I. Mohamed, M. Abdalla, and A. E.-A. Mitkees, "Perfect isolation performance among two-element MIMO antennas," *AEU-Int. J. Electron. Commun.*, vol. 107, pp. 21–31, Jul. 2019.
[18] K.-D. Xu, H. Luyen, and N. Behdad, "A decoupling and matching network design for single- and dual-band two-element antenna arrays," *IEEE Trans. Microw. Theory Techn.*, vol. 68, no. 9, pp. 3986–3999, Sep. 2020.
[19] Z. Niu, H. Zhang, Q. Chen, and T. Zhong, "Isolation enhancement in closely coupled dual-band MIMO patch antennas," *IEEE Antennas Wireless Propag. Lett.*, vol. 18, no. 8, pp. 1686–1690, Aug. 2019.
[20] K.-L. Wu, C. Wei, X. Mei, and Z.-Y. Zhang, "Array-antenna decoupling surface," *IEEE Trans. Antennas Propag.*, vol. 65, no. 12, pp. 6728–6738, Dec. 2017.
[21] M. Li, B. G. Zhong, and S. W. Cheung, "Isolation enhancement for MIMO patch antennas using near-field resonators as coupling-mode transducers," *IEEE Trans. Antennas Propag.*, vol. 67, no. 2, pp. 755–764, Feb. 2019.
[22] H. Lin, Q. Chen, Y. Ji, X. Yang, J. Wang, and L. Ge, "Weak-field-based self-decoupling patch antennas," *IEEE Trans. Antennas Propag.*, vol. 68, no. 6, pp. 4208–4217, Jun. 2020.
[23] T. Hassan, M. U. Khan, H. Attia, and M. S. Sharawi, "An FSS based correlation reduction technique for MIMO antennas," *IEEE Trans. Antennas Propag.*, vol. 66, no. 9, pp. 4900–4905, Sep. 2018.
[24] J.-F. Qian, F.-C. Chen, Q.-X. Chu, Q. Xue, and M. J. Lancaster, "A novel electric and magnetic gap-coupled broadband patch antenna with improved selectivity and its application in MIMO system," *IEEE Trans. Antennas Propag.*, vol. 66, no. 10, pp. 5625–5629, Oct. 2018.
[25] G. Kumar and K. Gupta, "Broad-band microstrip antennas using additional resonators gap-coupled to the radiating edges," *IEEE Trans. Antennas Propag.*, vol. AP-32, no. 12, pp. 1375–1379, Dec. 1984.
[26] G. Kumar and K. Gupta, "Nonradiating edges and four edges gap-coupled multiple resonator broad-band microstrip antennas," *IEEE Trans. Antennas Propag.*, vol. AP-33, no. 2, pp. 173–178, Feb. 1985.
[27] S.-H. Wi, Y.-S. Lee, and J.-G. Yook, "Wideband microstrip patch antenna with U-shaped parasitic elements," *IEEE Trans. Antennas Propag.*, vol. 55, no. 4, pp. 1196–1199, Apr. 2007.
[28] Y. Cao, Y. Cai, W. Cao, B. Xi, Z. Qian, T. Wu, and L. Zhu, "Broadband and high-gain microstrip patch antenna loaded with parasitic mushroom-type structure," *IEEE Antennas Wireless Propag. Lett.*, vol. 18, no. 7, pp. 1405–1409, Jul. 2019.

HUY HUNG TRAN received the B.S. degree in electronics and telecommunications from the Hanoi University of Science and Technology, Hanoi, Vietnam, in 2013, the M.S. degree from Ajou University, Suwon, South Korea, in 2015, and the Ph.D. degree from Dongguk University, Seoul, South Korea, in 2020. His current research interests include circularly polarized antennas, high gain antennas, metamaterial based antennas, and reconfigurable antennas.

NGHIA NGUYEN-TRONG (Member, IEEE) received the Ph.D. degree in electrical engineering from The University of Adelaide, Adelaide, SA, Australia, in 2017.

He worked as a Postdoctoral Research Fellow with The University of Queensland, QLD, Australia, from 2017 to 2020. He is currently a Lecturer with The University of Adelaide. His current research interests include leaky-wave antennas, monopolar antennas, Fabry–Perot antennas, and reconfigurable antennas.

Dr. Nguyen-Trong was one of the recipients of the Best Student Paper Award at the 2014 IWAT, the 2015 IEEE MTT-S NEMO, and the 2017 ASA Conferences, and the Best Paper Award at the 2018 and 2020 AMS Conference. He has been continuously selected as a Top Reviewer for IEEE TRANSACTIONS ON ANTENNAS AND PROPAGATION (TAP), in 2018, 2019, and 2020, and IEEE ANTENNA WIRELESS AND PROPAGATION LETTER, in 2018. He serves as the Technical Chair for the 2020 Australian Microwave Symposium (AMS).